IX International Conference on Particle-Based Methods
PARTICLES 2025
J. Bonet, M. Cremonesi, A. Franci, A. Gil (Eds)

IMPACT OF OUTLET BOUNDARY CONDITION SCHEMES FOR THE LATTICE BOLTZMANN METHOD REGARDING THE STEFAN PHASE-CHANGE PROBLEM

IVAN T. MARTINS[*,†], LUBEN C. GÓMEZ[*] AND PABLO F. ALVARIÑO[†]

* Thermal and Fluid Engineering Laboratory (LETeF)
University of São Paulo (USP), São Carlos School of Engineering (EESC)
Av. Trabalhador Sao-carlense 400, 13561-250, São Carlos, Brazil

† Grupo de Investigación en Sistemas Térmicos y Transferencia de Calor (SISTER)
Universidade da Coruña (UDC), Campus Industrial de Ferrol
Rúa Mendizábal s/n, 15403, Ferrol, Spain

Key words: Lattice Boltzmann Method, Outflow Boundary Condition, Multiphase Flows, Boiling Simulation, Phase-field LBM.

Abstract. In several industrial applications, there are systems that depend on multiphase flows. Consequently, modelling these processes are very attractive for the scientific community. Having a mesoscopic nature, the lattice Boltzmann method (LBM) presents advantages to deal with complex geometries and complex processes, such as bubble merging, fluid-structure interaction, etc. Several LBM models for multiphase flows were developed by the research community. Usually, in the applications of multiphase flows, there are open boundaries where the fluid with more than one phase leaves the domain. However, there are few works in the literature regarding the impact of the BC schemes with the Allen-Cahn-based phase-field LBM, especially considering liquid-gas phase change. Then, in this work, we explore the impact of three schemes of open BC: the equilibrium scheme, the extrapolation scheme, and the convective BC scheme. First, the impact of the BC schemes on a channel flow with a bubble inside is studied. Next, the Stefan problem considering real properties (saturated HFE7100) is simulated. The results showed that both the extrapolation and equilibrium schemes can introduce instabilities and incoherences in the results, while the convective BC is the one that better conserves the coherence of the results.

1 INTRODUCTION

As many engineering applications involve fluid flow through channels or open boundaries, the correct implementation of outflow boundary conditions (BCs) is of utmost importance for the correct modeling and simulation of those devices, including multiphase flows. Regarding this kind of flows, there are several methods in the literature developed to handle it, but it is still an open research issue. Among them, the lattice Boltzmann method (LBM) presents some attractive characteristics to deal with multiphase flows, such as its mesoscopic nature, which facilitates the simulation of complex interfacial movements, for example [1].

In the subject of two-phase flows with phase-change, several LBM models were developed for this application, such as the color-gradient model, pseudopotential method, the free energy LBM, and the phase-field methods. In the scope of phase-field LBM, recently Martins et al. [2] have proposed an Allen-Cahn-based LBM for simulating liquid-gas flows with phase-change. However, as observed by the authors, the outflow BC scheme for these applications needs careful attention.

Lu et al. [3] were one of the pioneers in the study of outflow BC for phase-field LBM. The authors evaluated three schemes of outflow BC: the Neumann BC, the Convective BC, and the extrapolation BC applied to a droplet flow on a channel, with and without obstacles. They used the phase-field LBM developed by He et al. [4], popularly known as the HCZ model, and found that convective schemes already showed to be the best option for this kind of BC. In the field of other multiphase LBM models, Zong et al. [5] performed a study regarding the color-gradient LBM model, proposing a new outflow BC for this kind of model. Additionally, Wang et al. [6] had investigated two pressure BC for the pseudopotential LBM.

However, works on the impact of these BCs in the phase-field LBM considering the phase-change process are scarce. In this context, the present work investigates the behavior of three schemes of outflow BC: the extrapolation, the equilibrium, and the convective methods, applied to liquid-gas phase-change problems with a phase-field LBM. For this task, first, an isothermal multiphase flow is addressed considering a liquid stream with one bubble. The analysis ends with the evaluation of the three BC schemes for the Stefan problem: a one-dimensional case with phase-change. The analysis is performed considering both density contours visualization, mass conservation analysis, and comparison with reference solutions, in the case of the Stefan problem.

2 METHODOLOGY

The analysis performed in this paper employs the LBM model proposed by Martins et al. [2], which consists of an Allen-Cahn-based LBM for thermal liquid-gas phase change simulation. Here, it is important to highlight that this model uses the dimensional approach proposed by Martins et al. [7], which avoids the necessity of using lattice units, and all variables are implemented directly in physical units in the simulation. This facilitates the consideration of real operational conditions and real fluids in our analysis. In this section, a brief explanation of the method is provided. More information can be found in Martins et al. [2].

The method uses three distribution functions: one for tracking the liquid-gas interface through the order parameter, f_i, another for modeling the fluid pressure and velocity, g_i, and a third one for the temperature field, s_i. The lattice Boltzmann equations (LBEs) for each distribution function are depicted in Eqs. (1),(2) and (3), where the interface tracking and the energy conservation LBEs use the BGK collision operator, while the momentum LBE benefits from the MRT collision operator, to increase the stability of the method. The variables S are the source terms for each LBE, which are defined below in this section.

$$f_i(\mathbf{x}+\mathbf{c_i}\Delta t, t+\Delta t) - f_i(\mathbf{x},t) = -\frac{\Delta t}{\tau_\phi}\left[f_i(\mathbf{x},t) - f_i^{eq}(\mathbf{x},t)\right] + \left(1-\frac{\Delta t}{2\tau_\phi}\right) S_{f_i}(\mathbf{x},t)\Delta t \quad (1)$$

$$\begin{aligned} g_i(\mathbf{x}+\mathbf{c}_i\Delta t, t+\Delta t) - g_i(\mathbf{x},t) = -\Delta t\left[\mathbf{M}^{-1}\mathbf{\Lambda}\mathbf{M}\right]_{ij}\left[g_j(\mathbf{x},t) - g_j^{eq}(\mathbf{x},t)\right] + \\ \Delta t\mathbf{M}_{ij}^{-1}\left(I_{ij} - \frac{\Delta t\mathbf{\Lambda}_{ij}}{2}\right)\mathbf{S}_{g_j}(\mathbf{x},t) \end{aligned} \quad (2)$$

$$s_i(\mathbf{x}+\mathbf{c_i}\Delta t, t+\Delta t) - s_i(\mathbf{x},t) = -\frac{\Delta t}{\tau_T}\left[s_i(\mathbf{x},t) - s_i^{eq}(\mathbf{x},t)\right] + \left(1-\frac{\Delta t}{2\tau_T}\right) S_{s_i}(\mathbf{x},t)\Delta t \quad (3)$$

In these equations, τ are the relaxation rates for each equation, $\mathbf{c}_i$ are the discrete velocities for each direction i, which depend on the velocity scheme chosen. $\mathbf{M}$ is the transformation matrix, while $\mathbf{\Lambda}$ is the collision matrix, both for the MRT collision operator (for more information, see Martins et al. [2]). The superscript eq indicates the equilibrium distribution functions, which for the interface tracking and energy LBEs are defined by Eq. (4), while the equilibrium moments for the momentum conservation equation are given by Eq. (5), considering the D2Q9 velocity scheme [8]. In these equations, w_i are the weights, which depends on the velocity scheme, c_s is the sound speed, $\mathbf{u} = (u, v)$ is the fluid local velocity, ϕ is the order parameter (or liquid concentration) and T is the relative temperature, defined as $T = T_{absolute} - T_{sat}$, where T_{sat} is the saturation temperature. $p = P_{absolute} - P_{sat}$ is the relative pressure and $c = \Delta x/\Delta t$ is the lattice speed.

$$h_i^{eq} = w_i\phi\left[1 + \frac{\mathbf{c}_i\cdot\mathbf{u}}{c_s^2}\right] \;\; ; \;\; s_i^{eq} = w_i T\left[1 + \frac{\mathbf{c}_i\cdot\mathbf{u}}{c_s^2}\right] \quad (4)$$

$$\begin{aligned} \mathbf{m}^{eq} = \left\{0;\; 3\left(\rho\mathbf{u}\cdot\mathbf{u} + 2p\right);\; -3c^2\left(\rho\mathbf{u}\cdot\mathbf{u} + 3p\right);\; \rho u;\; -c^2\rho u;\; \rho v;\; -c^2\rho v;\right. \\ \left.\rho\left(u^2 - v^2\right);\; \rho uv\right\} \end{aligned} \quad (5)$$

Treating the source terms, they can be defined by Eqs. (6), (7) and (8), where $\dot{m}'''$ is the vapor generation term, $\mathbf{F} = (F_x, F_y)$ are the external forces acting in the domain, which here consist only of the interfacial force, defined by $\mathbf{F}_i = \mu_\phi\nabla\phi$. μ_ϕ is the chemical potential, defined as $\mu_\phi = 4\beta\left(\phi-1\right)\left(\phi-0.5\right) - \kappa\nabla^2\phi$, where β and κ are constants related to the fluid surface tension, σ, and interface width W, as $\beta = 12\frac{\sigma}{W}$ and $\kappa = \frac{3}{2}\sigma W$.

$$S_{f_i} = w_i\left\{\frac{\mathbf{c_i}\cdot\left[\partial_t(\phi\mathbf{u}) + c_s^2\frac{4\phi(1-\phi)}{W}\mathbf{n}\right]}{c_s^2} - \frac{\dot{m}'''}{\rho_l}\right\} \quad (6)$$

$$\begin{aligned}\mathbf{S_g} = \{&\nabla\rho\cdot\mathbf{u} + \rho\dot{m}'''\left(\rho_g^{-1}-\rho_l^{-1}\right);\\ &-2c^2\rho\dot{m}'''\left(\rho_g^{-1}-\rho_l^{-1}\right);\ c^4\left[\rho\dot{m}'''\left(\rho_g^{-1}-\rho_l^{-1}\right)-\nabla\rho\cdot\mathbf{u}\right];\\ &F_x;\ -c^2F_x;\ F_y;\ -c^2F_y;\ \frac{2}{3}c^2\left(u\partial_x\rho - v\partial_y\rho\right);\ \frac{1}{3}c^2\left(v\partial_x\rho + u\partial_y\rho\right)\}\end{aligned} \tag{7}$$

$$S_{s_i} = w_i\left[\frac{\mathbf{c_i}\cdot\partial_t\left(T\mathbf{u}\right)}{c_s^2} + T\dot{m}'''\left(\rho_g^{-1}-\rho_l^{-1}\right)\right] \tag{8}$$

The vapor generation term is related to the liquid conductivity, k_l, to the latent heat of vaporization, h_{lg}, and to a correction constant, K, which for the present operational conditions is $K = 6.2$ [2].

$$\dot{m}''' = K\frac{k_l\nabla T\cdot\nabla\phi}{h_{lg}} \tag{9}$$

The macroscopic variables can be recovered from the moments of the distribution functions. The order parameter can be obtained from Eq. (10), while the local density can be obtained from a linear interpolation of ϕ: $\rho = \phi\rho_l + (1-\phi)\rho_g$. The same rule is applied for the local conductivity, local specific heat, and local dynamic viscosity. The macroscopic pressure and momentum can be calculated through Eqs. (11) and (12), respectively, and the temperature, by Eq. (13). The temporal and spatial gradients are approximated by finite difference schemes as in [2].

$$\phi = \sum_{i=0}^{q-1} f_i - \frac{\Delta t}{2}\frac{\dot{m}'''}{\rho_l} \tag{10}$$

$$p = \frac{c_s^2}{1-w_0}\left\{\sum_{i\neq 0}^{q-1} g_i + \rho w_0\left[-\frac{\mathbf{u}\cdot\mathbf{u}}{2c_s^2}\right] + \frac{\Delta t}{2}\left[\mathbf{u}\cdot\nabla\rho + (1-w_0)\,\rho\dot{m}'''\left(\frac{1}{\rho_g}-\frac{1}{\rho_l}\right)\right]\right\} \tag{11}$$

$$\rho\mathbf{u} = \sum_{i=0}^{q-1}\mathbf{c_i}g_i + \frac{\Delta t}{2}\mathbf{F} \tag{12}$$

$$T = \left[1 - \frac{\Delta t}{2}\dot{m}'''\left(\rho_g^{-1}-\rho_l^{-1}\right)\right]^{-1}\sum_{i=0}^{q-1} s_i \tag{13}$$

2.1 Schemes for outlet boundary condition

In this work, we explore three main propositions of the scheme for the outflow boundary condition: the extrapolation method, the equilibrium method, and the convective method. Starting with the extrapolation method, the unknown functions at the boundary node, $\mathbf{x_b}$, are calculated

by extrapolating from the functions of the neighbor nodes, $\mathbf{x_b} - \Delta x \mathbf{n}$, as given by Eq. (14). In this equation, $\mathbf{n}$ is the normal vector, pointing into the domain.

$$f_i(\mathbf{x_b}, t + \Delta t) = f_i(\mathbf{x_b} - \Delta x \mathbf{n}, t + \Delta t) \qquad g_i(\mathbf{x_b}, t + \Delta t) = g_i(\mathbf{x_b} - \Delta x \mathbf{n}, t + \Delta t) \quad (14)$$

The equilibrium scheme assumes that the unknown populations are in equilibrium with the imposed variables at the boundary, such as pressure, velocity, or density/order parameter. Usually, the velocity value at the boundary is unknown, and an extrapolation can be made to estimate it. In our case, we will extrapolate from the neighbor node, $\mathbf{u}_b \approx \mathbf{u}(\mathbf{x_b} - \Delta x \mathbf{n}, t + \Delta t)$. This condition can be represented by Eq. (15).

$$f_i(\mathbf{x_b}, t + \Delta t) = f_i^{eq}(\mathbf{u_b}, \phi_b) \qquad g_i(\mathbf{x_b}, t + \Delta t) = g_i^{eq}(\mathbf{u_b}, \rho_b, p_b) \quad (15)$$

The last scheme of boundary condition considered here is the convective scheme. In this case, a characteristic velocity, U, is defined, and all the distribution functions, as well as the unknown variables for gradient calculation at the boundary (ϕ), are calculated using this velocity and from the neighborhood. According to Lou et al. [3], this convective velocity can be calculated by averaging the u component of $\mathbf{u}(\mathbf{x_b} - \Delta x \mathbf{n}, t + \Delta t)$ in the y direction: $U = N^{-1} \sum_y u_{x,y}(\mathbf{x_b} - \Delta x \mathbf{n}, t + \Delta t)$, where N is the number of nodes in y direction. After that, the unknown functions can be calculated using Eq. (16).

$$\begin{aligned} f_i(\mathbf{x_b}, t + \Delta t) &= \frac{f_i(\mathbf{x_b}, t) + U f_i(\mathbf{x_b} - \Delta x \mathbf{n}, t + \Delta t)}{1 + U} \\ g_i(\mathbf{x_b}, t + \Delta t) &= \frac{g_i(\mathbf{x_b}, t) + U g_i(\mathbf{x_b} - \Delta x \mathbf{n}, t + \Delta t)}{1 + U} \end{aligned} \quad (16)$$

3 RESULTS

3.1 Bubble flow

The first problem to be studied is an isothermal channel with liquid flow through a bubble, initially placed near the entrance of the channel. In this case, we used a pseudofluid, whose properties are a density of $\rho_l^* = 1000$ and a kinematic viscosity of $\nu_l^* = 0.1$ for the liquid phase, while the respective properties for the gas phase are $\rho_g^* = 100$ and $\nu_g^* = 0.001$. The surface tension between the phases was $\sigma^* = 0.001$ and the mobility was $M = 0.10$. The interface width was chosen to be $W^* = 5$ lattice units (l.u.). The initial radius of the bubble was 25 l.u., placed at the y-center of the channel, at 70 l.u. from the channel entrance. For the inlet velocity, a uniform profile with $u_{in}^* = 0.010$ was implemented. The channel dimensions were 200 l.u. in the x direction and 100 l.u. in the y direction.

The bounce-back rule [9] was used to implement the stationary walls at the top and bottom of the channel, as well as for the inlet velocity at the left boundary of the domain. The right boundary consists of the outlet BC, which was implemented using the three BC schemes: the

extrapolation method, the equilibrium, and the convective BCs, which are the main focus of this study. The main goal here is to investigate the behavior of these three BC schemes, considering the mass conservation of the domain and additional effects in the multiphase fluid streams.

The simulation was run up to 12000 time steps. The density contours for each outlet BC are shown in Fig. 2 for four different time steps, ranging from the start of the bubble movement to the complete exit of the gas phase of the channel. The figures show that, during the bubble motion, both the convective and the extrapolation methods cause a similar deformation of the bubble, while the equilibrium scheme introduces some additional suction effects, stretching the bubble (see $t^* = 6000$ in Fig. 1c).

When the bubble reaches the outlet boundary, the equilibrium scheme stops converging and diverged throughout the entire simulation. The divergent results are represented as full blue channels in Fig. 1d and 1e. At $t^* = 9000$, the bubble profile for the extrapolation BC starts to deviate from the convective BC profile, presenting a smoother shape with lower tails in comparison to the convective BC bubble. After the entire bubble passed the outlet boundary, the convective BC was the only condition that remained stable, while the extrapolation method starts to introduce some non-physical gas formation through the entire domain, as we can see in Fig. 1e. From this analysis, we can already conclude that the extrapolation and the equilibrium schemes can not handle multiphase flow when using the Allen-Cahn-based LBM.

To give an additional perspective about the behavior of the three BC schemes, the total mass of the domain was calculated for each time step, represented in Fig. 2. As the Allen-Cahn-based LBM here assumes that each phase is incompressible, we only expect a variation of the domain density after the bubble reaches the outlet of the channel. As the volume occupied by the bubble with density $\rho_g^* < \rho_l^*$ is filled with liquid, a slight increase in the total mass of the domain is expected. Defining the initial mass of the domain as $m_i = (\forall_{domain} - \forall_{bubble})\rho_l + \forall_{bubble}\rho_g$ and the final mass of the domain as $m_i = \forall_{domain}\rho_l$, the total mass change after the full exit of the bubble should be $\Delta m = \forall_{bubble}(\rho_l - \rho_g)$. Then, we have $\Delta m/m_i = \forall_{domain}/[\forall_{bubble}(1-\rho_g/\rho_l)]$. Considering the domain of 200:100, a bubble with radius of 25 and the liquid and gas density mentioned before, we have $\Delta m/m_i = 11\%$. Thus, after the exit of the bubble, we expect the final domain mass to be 11% higher.

Examining Fig. 2, first we can see that the three BC schemes experienced a slight initial increase in the domain mass, between $2\% - 2.5\%$ of the initial mass. This can be due to the numerical accommodation of the phases, which are trying to reach an equilibrium state that is different from the initialized profile. This could be avoided by initializing exactly with the expected equilibrium profile, which is not a simple task. After that, the mass of the domain is almost constant for the three schemes, presenting little differences between the stable values, which represent the bubble motion through the channel. Close to $t^* = 7500$, the bubble reaches the outlet boundary, represented by the growing trend observed in the three curves. The case with the equilibrium BC diverges fast after the start of the bubble exit, while the two other schemes still present converging results.

However, after the full exit of the bubble (about $t^* = 1000$), the case with the extrapolation condition presents a fast decay of the domain mass, indicating that the gas formation observed

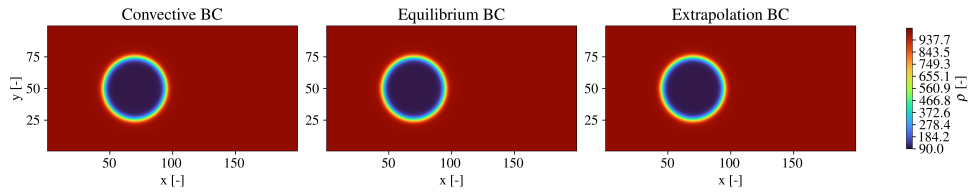

(a) t* = 0

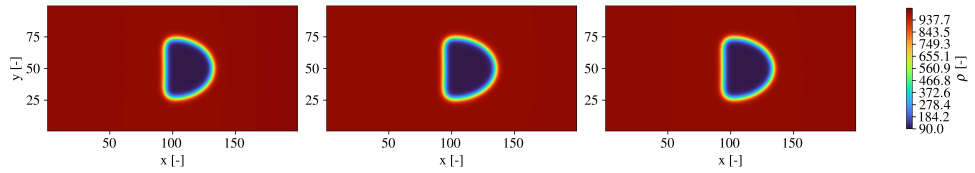

(b) t* = 3000

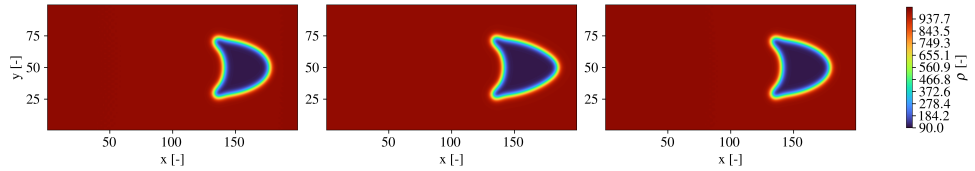

(c) t* = 6000

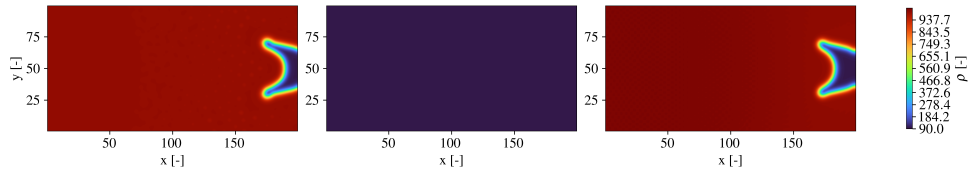

(d) t* = 9000

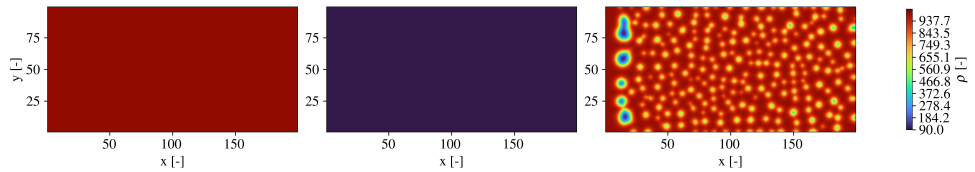

(e) t* = 12000

Figure 1: Density contours for each tested BC for different time steps.

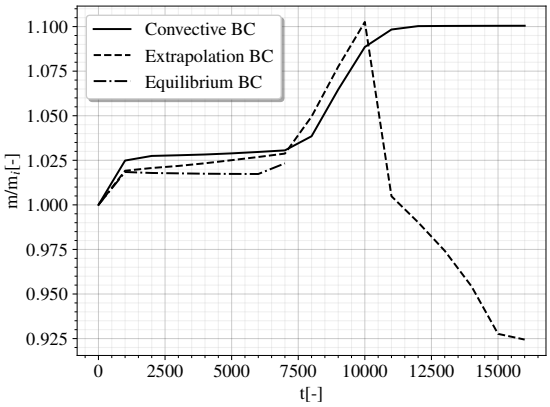

Figure 2: Temporal evolution of total domain mass in relation to the initial mass.

in Fig. 1e starts. On the other hand, the convective BC allowed the simulation to reach a stable condition, evidenced by the horizontal step reached after $t^* = 10000$. In addition, for this BC scheme, the final domain mass is about 10% of the initial mass, which is close to the 11% expected theoretically. This final remark allows the conclusion that among the studied BC schemes, the convective one is the best for multiphase flow, guaranteeing also mass conservation in a satisfactory way.

3.2 Stefan Problem

The next problem consists of a non-isothermal case with phase change: the Stefan problem. It consists of a 1D phase change problem, where saturated liquid is in contact with a superheated wall at the left boundary, which causes the liquid to evaporate, while the right boundary is left open (where the outflow BC is tested, in this case). Having an analytical solution, it is a common benchmark exercise for verifying numerical methods for phase-change [11–13]. The analytical solution for the liquid-gas interface position, $x_i(t)$, and velocity, $u_i(t)$, are given by Eq. (17), where λ is the solution of the following equation: $\lambda e^{\lambda^2}\text{erf}(\lambda) = St/\sqrt{\pi}$. In these equations, $St = c_{p,g}\Delta T/h_{lg}$ is the Stefan number and $\alpha_g = k_g/(\rho_g c_{p,g})$ is the gas thermal diffusivity.

$$x_i(t) = 2\lambda\sqrt{\alpha_g t} \quad ; \quad u_i(t) = \lambda\sqrt{\frac{\alpha_g}{t}} \tag{17}$$

Unlike in the previous section, here we are considering real fluids under real operational conditions: saturated HFE7100 fluid at 195kPa with a wall superheating of 5.1 K. The properties under these operational conditions are $\rho_l = 1355.72kg\ m^{-3}$ and $\rho_g = 18.09kg\ m^{-3}$ for the densities, $\mu_l = 3.15 \cdot 10^{-4}Pa\ s$ and $\mu_g = 0.21 \cdot 10^{-4}Pa\ s$ for the dynamic viscosities, $k_l = 5.76 \cdot 10^{-2}W\ m^{-1}K^{-1}$ and $k_g = 0.98 \cdot 10^{-2}W\ m^{-1}K^{-1}$ for the thermal conductivity, $c_{p,l} = 1228.76J\ kg^{-1}K^{-1}$ and $c_{p,g} = 974.05J\ kg^{-1}K^{-1}$ for the specific heat, a surface tension of $\sigma =$

$0.0077N/m$, a latent heat of vaporization of $h_{lg} = 108880.64J\ kg^{-1}$ and a thermal expansion coefficient of $\beta_T = 2.31 \cdot 10^{-3}K^{-1}$.

The domain length was 2.5 mm, and, in this case, the D1Q3 scheme was used instead of D2Q9 (as in the last section). The time and space discrete intervals were adopted as $\Delta t = 0.25 \cdot 10^{-6}s$ and $\Delta x = 5 \cdot 10^{-6}m$, respectively. The mobility was chosen as $M = 1 \cdot 10^{-5}m^2s^{-1}$, with an interface width of $W = 5\Delta x = 25\mu$m . An initial layer of vapor was initialized on the left of the domain, with an initial interface position of $x_i = 0.15mm$. The initial density profile was generated considering a hyperbolic tangential profile, as in Martins et al. [2].

In terms of fluid BC, the left boundary was treated as a rigid wall, implemented with the bounce back rule. The right boundary was implemented considering the three BC schemes discussed for open boundaries for f_i and g_i. From the thermal point of view, the left wall was kept at a constant temperature of $T_w = T_{sat} + \Delta T$, where $T_{sat} = 355.4K$ is the saturation temperature at 195kPa and $\Delta T = 5.1K$ is the superheating degree. The anti-bounce-back rule [10] was used to implement this condition, Eq. (14). The right wall was implemented with the extrapolation BC for the temperature distribution function (s_i).

Figure 3 gives the interface position and velocity with time for each outlet BC scheme, in comparison to the analytical solution. The first thing to be observed is that the extrapolation BC was not able to keep the simulation stable, diverging from the early stages of the simulation. In an attempt to get more stability, larger domains were also tested with this BC. Besides, we have observed that some intermediate values of L could stabilize the simulation for a longer period of time, but all of them diverge at the end. Then, differently from what is found in sec. 3.1, where the extrapolation BC only diverges after the gas phase comes in contact with the outlet BC, here it diverges since the beginning, even having only liquid at the outlet boundary.

Meanwhile, both the equilibrium and the convective BC were able to simulate the Stefan problem, presenting good results in comparison to the analytical solution. One can note that, despite presenting good results for the Stefan problem, this behavior was not observed in the previous case (sec. 3.1) for the equilibrium scheme. As we observed before, the equilibrium BC diverged when the gas phase had reached the outflow boundary. For the Stefan problem, as in our case, the gas phase does not reach the exit of the domain for the total simulated time (about 9 s), and the equilibrium BC remained stable. Thus, even this scheme presented good results for the Stefan problem, we should be aware that this kind of BC for outlets can cause instabilities if the gas phase reaches the outlet boundary, as observed before. Again, convective BC was presented as the best option for the outlet BC.

As a final analysis, the evolution of the total mass of the domain with time was compared between the analytical prediction and the numerical results. The mass conservation law applied to the Stefan problem can be reduced to $\dot{m} = -\rho_l u_l A_{out}$, where u_l is the liquid velocity ($u_l = u_i(1 - \rho_g/\rho_l)$) and A_{out} is the transverse section outlet area. This results in the following equation for the mass of the domain over time: $m(t) = m_i - A_{out}(\rho_l - \rho_g)x_i(t)$.

Taking as reference time the beginning of the simulation, the equivalent time t_i to have an initial interface position of 0.15 mm, the comparison between the analytical solution and the numerical results for each BC scheme is depicted in Fig. 4. The first thing that one can

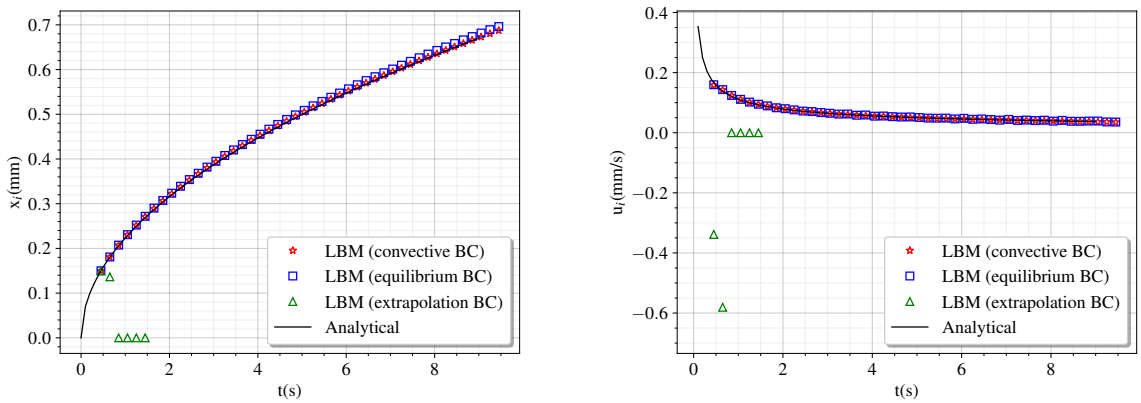

Figure 3: Interface position (a) and velocity (b) with time for the Stefan problem, considering the three tested BC schemes and the analytical solution.

realize is that, before destabilizing, the extrapolation BC presents a mass increment, which is neither expected nor verified in any other tested condition. Additionally, both the equilibrium and convective BC presented very good solutions in comparison to the analytical one, with the results for the convective BC closer to the analytical than the results for the equilibrium scheme. This final analysis only confirms what was already discussed before: that the convective scheme is the most suitable for dealing with outflow BC, presenting both stable and accurate results.

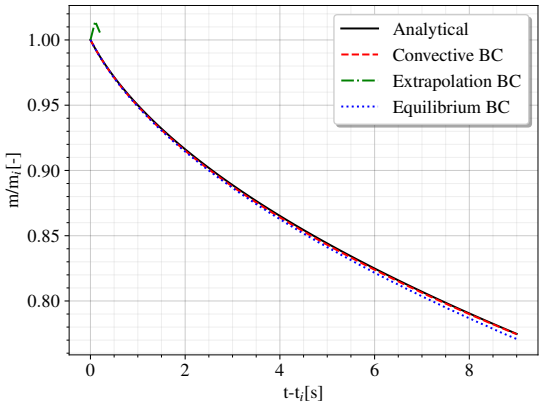

Figure 4: Temporal evolution of total domain mass in relation to the initial mass for the Stefan problem, considering the three tested BC schemes and the analytical solution.

4 CONCLUSIONS

The present work performed a study regarding three different schemes of implementation for the outlet BC, considering the Allen-Cahn-based LBM with phase-change. Three schemes were considered: the extrapolation, the equilibrium, and the convective methods. First, an isothermal problem of bubble blow in a channel was tested. Next, the Stefan problem was the object of study, consisting of a 1D phase-change problem with an open boundary condition at the right boundary.

The results for the bubble flow evidenced that the equilibrium scheme is not capable of handling two-phase flows crossing the outlet boundary. It destabilizes and diverges the method by the moment that the other phase of the domain (in our case, the gas phase) reaches the outlet. Considering the extrapolation method, it also destabilizes the simulations, because at the instant that the bubble leaves the domain completely, small amounts of vapor start to appear throughout the entire domain, leading to convergence problems. The only scheme that was able to handle this kind of problem was the convective BC, also showing a satisfactory agreement with the mass conservation of the domain.

Regarding the Stefan problem, the extrapolation BC destabilized the simulation since early stages, presenting an unexpected increase in the domain mass at the beginning of the simulation. On the other hand, both equilibrium and convective BC presented very good results. Both the interface position and velocity, as well as, the mass conservation of the domain, were in very good agreement with the analytical solution.

The results analyzed in this work elucidate that the convective scheme is the best in terms of stability and accuracy to deal with outflow BC, considering the three BC schemes studied here. Besides the equilibrium BC showed good results for the Stefan problem, it was not capable of simulating a bubble flow in a liquid channel. At the same time, the extrapolation BC presented stability issues in both tested cases.

ACKNOWLEDGMENTS

This study was financed by the São Paulo Research Foundation (FAPESP), Brasil, process numbers #2021/14338-0, #2022/15765-1, #2023/02383-6, and #2024/21322-0. The authors also acknowledge the support received from CNPq (National Council for Scientific and Technological Development, process 305771/2023-0).

REFERENCES

[1] Mohamad, A.A. *Lattice Boltzmann Method: Fundamentals and Engineering Applications with Computer Codes.* Springer-Verlag London Ltd., Vol. II (2019).

[2] Martins, I.T., Gómez, L.C. and Alvariño, P.F. “Design and validation of a lattice Boltzmann method with real properties for single-bubble boiling simulation.” *Int. J. Commun. in Heat and Mass Transf.* (2025) 167:109207.

[3] Lou, Q., Guo, Z., Shi, B. “Evaluation of outflow boundary conditions for two-phase lattice

Boltzmann equation." *Phys. Rev. E.* (2013) 87:063301.

[4] He, X., Chen, S., Zhang, R. "A Lattice Boltzmann Scheme for Incompressible Multiphase Flow and Its Application in Simulation of Rayleigh–Taylor Instability." *J. Comp. Phys.* (1999) 152:642.

[5] Zong, Y., Li, M., Wang, K. "Outflow boundary condition of multiphase microfluidic flow based on phase ratio equation in lattice Boltzmann method." *Phys. Fluid.* (2021) 33:073304.

[6] Wang, Z., Soomro, M., Peng, C., Ayala, L. F., Ayala, O. M. "Two pressure boundary conditions for multi-component multiphase flow simulations using the pseudo-potential lattice Boltzmann model." *Comp. & Fluid.* (2022) 248:105672.

[7] Martins, I.T., Alvariño, P.F. and Gómez, L.C. "Lattice Boltzmann method for simulating transport phenomena avoiding the use of lattice units." *J. Braz. Soc. Mech. Sci.* (2024) 46:333.

[8] Qian,Y. H., D'Humières, D., Lallemand, P. "Lattice BGK Models for Navier-Stokes Equation." *Europhys. Lett.* (1992) 17(6):479.

[9] Ladd, A.J. "Numerical Simulations of Particulate Suspensions Via a Discretized Boltzmann Equation. Part 1. Theoretical Foundation." *J. Fluid Mec.* (1994) 271:285.

[10] Ginzburg, I. "Generic boundary conditions for lattice Boltzmann models and their application to advection and anisotropic dispersion equations." *Adv. Water Resour.* (2005) 28:1196.

[11] Fogliatto, E. O., Clausse, A., Teruel, F. E. "Development of a double-MRT pseudopotential model for tridimensional boiling simulation." *Int. J. Therm. Sci.* (2022) 179:107637.

[12] Saito, S., De Rosis, A., Fei, L., Luo, K.H., Ebihara, K.-I., Kaneko, A., Abe, Y. "Lattice Boltzmann modeling and simulation of forced-convection boiling on a cylinder." *Phys. Fluid.* (2021) 33(2):109207.

[13] Mirhoseini, M., Banaee, A., Jalali, A."A novel phase-field lattice Boltzmann framework for diffusion-driven multiphase evaporation." *Phys. Fluid.* (2021) 36(8):083314.